Implementable Space Mapping Approach to Enhancement of Microwave Device Models

John W. Bandler*, Fellow, IEEE*, Qingsha S. Cheng*, Member, IEEE*, and Slawomir Koziel*, Member*, *IEEE*

McMaster University, Hamilton, ON, L8S4K1, Canada www.sos.mcmaster.ca

Abstract—**We present advances in microwave and RF device modeling exploiting the Space Mapping (SM) technology. New SM-based modeling techniques are proposed that are easy to implement entirely in the Agilent ADS framework. This makes the SM modeling concept available to engineers through widely used commercial software. It permits the creation of library models that can be used for model enhancement of microwave elements. A set of four different SM-based models is presented along with corresponding implementations in the ADS schematic for a microstrip right-angle bend and a microstrip shaped T-junction. Fine model data is obtained from Sonnet's *em*.**

Index Terms—**CAD, optimization, EM modeling, microstrip modeling, microwave filters, space mapping, surrogate modeling.**

I. INTRODUCTION

Space Mapping (SM) technology [1], [2], [3] addresses the issue of reducing unnecessary time-consuming full-wave EM simulations of microwave structures in device modeling problems and design optimization.

SM assumes the existence of "fine" and "coarse" models. The "fine" model may be a CPU-intensive EM simulator that provides high accuracy. The "coarse" model is a simplified representation, typically an equivalent circuit with empirical formulas. Modeling implementations of SM exploit the computational efficiency of coarse models and the accuracy of corresponding fine models so as to realize fast and accurate (enhanced) models valid in a wide range of the parameter spaces. Space derivative mapping [4], the so-called generalized SM [5] and SM-based neuromodeling [6,7] are three approaches.

It is desirable to engineers that SM-based models can be set up and used in connection with (or even within) available commercial software. Our paper explores this possibility. We consider a family of models that is implemented entirely in the Agilent ADS [8] framework. The models can be used as library models for corresponding microwave elements and hence for direct CAD and optimization.

II. MODEL DESCRIPTION

Let $R_f : X_f \to R^m$ and $R_c : X_c \to R^m$ denote the fine and coarse model response vectors, where $X_f \subseteq R^n$ and $X_c \subseteq R^n$ are design variable domains of the fine and coarse models, respectively. For example, $R_f(x)$ and $R_c(x)$ may represent magnitudes of a microwave filter transfer function at m chosen frequencies.

We denote by $X_R \subseteq X_f$ the region of interest in which we want enhanced matching between the surrogate and the fine model. We assume that X_R is an n-dimensional interval in R^n with center at reference point $x^0 = [x_{0.1} \ldots x_{0.n}]^T \in R^n$:

$$X_R = [x^0 - \delta, x^0 + \delta] = [x_{0.1} - \delta_1, x_{0.1} + \delta_1] \times \ldots \times [x_{0.n} - \delta_n, x_{0.n} + \delta_n] \quad (1)$$

where $\delta = [\delta_1 \ldots \delta_n]^T \in R_+^n$ determines the size of X_R. We use $X_R(x^0, \delta)$ to denote the region of interest defined by x^0 and δ.

The number of fine model evaluations used to construct a surrogate should be small since we assume that each evaluation is expensive. But, we have to account for dimension of the design variable space. We use the set of evaluation points (also called the *base set*) denoted by X_B, to consist of $2n+1$ points, where $n=\dim(X_f)$. We have

$$X_B = \{x^0, x^1, \ldots, x^{2n}\} \quad (2)$$

where x^0 is the reference point, and

$$x^j = x^0 + (-1)^j \delta_{\lceil j/2 \rceil} \cdot u_{\lceil j/2 \rceil}, \qquad j=1,\ldots,2n \quad (3)$$

where $u_k = [0 \ldots 0\ 1\ 0 \ldots 0]^T$ is a unit vector with 1 at the kth position; δ_k is the size of the region X_R along the kth axis. This distribution of points is called the star distribution [5].

Our basic SM-based surrogate model $R_{s1} : X_f \times M_{n \times n} \times M_{n \times 1} \to R^m$ ($M_{k \times l}$ denotes the set of $k \times l$ real matrices) is defined as

$$R_{s1}(x, \bar{B}, \bar{c}) = R_c(\bar{B} \cdot x + \bar{c}) \quad (4)$$

with matrices $\bar{B} \in M_{n \times n}$ and $\bar{c} \in M_{n \times 1}$ obtained by means of the parameter extraction

$$(\bar{B}, \bar{c}) = \arg \min_{(B,c)} \sum_{j=0}^{2n} \| R_f(x^j) - R_{s1}(x^j, B, c) \| \quad (5)$$

The model R_{s1} is based on the original space mapping concept [1].

The second model $R_{s2} : X_f \times M_{m \times m} \times M_{n \times n} \times M_{n \times 1} \to R^m$ is defined as

$$R_{s2}(x, \bar{A}, \bar{B}, \bar{c}) = \bar{A} \cdot R_c(\bar{B} \cdot x + \bar{c}) \quad (6)$$

with matrices $\bar{A} = diag\{a_1, \ldots, a_m\}$, $\bar{B} \in M_{n \times n}$ and $\bar{c} \in M_{n \times 1}$ obtained by means of the parameter extraction

$$(\overline{A}, \overline{B}, \overline{c}) = \arg\min_{(A,B,c)} \sum_{j=0}^{2n} \| R_f(x^j) - R_{s2}(x^j, A, B, c) \| \quad (7)$$

The model R_{s2} is based on the original SM and output SM (OSM) concepts [9].

The next model, $R_{s3} : X_f \times M_{n \times n} \times M_{n \times 1} \times M_{m \times 1} \to R^m$, also based on OSM, is defined as

$$R_{s3}(x, \overline{B}, \overline{c}, \overline{d}) = R_c(\overline{B} \cdot x + \overline{c}) + \overline{d} \quad (8)$$

Matrices $\overline{B} \in M_{n \times n}$, $\overline{c} \in M_{n \times 1}$, and $\overline{d} \in M_{m \times 1}$ are obtained using the parameter extraction

$$(\overline{B}, \overline{c}, \overline{d}) = \arg\min_{(B,c,d)} \sum_{j=0}^{2n} \| R_f(x^j) - R_{s3}(x^j, B, c, d) \| \quad (9)$$

The last model, $R_{s4} : X_f \times M_{m \times m} \times M_{n \times n} \times M_{n \times 1} \times M_{m \times 1} \to R^m$ is a combination of R_{s2} and R_{s3}. It is defined as

$$R_{s4}(x, \overline{A}, \overline{B}, \overline{c}, \overline{d}) = A \cdot R_c(\overline{B} \cdot x + \overline{c}) + \overline{d} \quad (10)$$

with matrices $\overline{A} = diag\{a_1, ..., a_m\}$, $\overline{B} \in M_{n \times n}$, $\overline{c} \in M_{n \times 1}$, and $\overline{d} \in M_{m \times 1}$ found using the parameter extraction

$$(\overline{A}, \overline{B}, \overline{c}, \overline{d}) = \arg\min_{(A,B,c,d)} \sum_{j=0}^{2n} \| R_f(x^j) - R_{s4}(x^j, A, B, c, d) \| \quad (11)$$

III. ADS IMPLEMENTATION

Unlike the optimization framework [10], our modeling implementation uses several points concurrently for parameter extraction. The SNP [8,10] file is awkward, however, Agilent provides an S2PMDIF (Multi-Dimensional 2-Port S-parameter File) component in the schematic. It "look(s) up" or "interpolate(s)" responses w.r.t. the desired parameters in Measurement Data Interchange Format (MDIF). The sets (base set or test set) of desired parameters are saved in a database file. They can be read by Data Access Component (DAC). We can use the Parameter Sweeps component to iterate through the parameters in the database file. Fig. 2 shows the ADS schematic setup of the fine model for multiple points. Using those components, a schematic can be set up to match surrogate responses to fine model responses.

ADS Schematic Modeling Framework for SM for Two-Ports

Step 1 Set up the fine model simulator, e.g., Sonnet *em* [11]; execute simulation using the base set points; save the responses in MDIF format.

Step 2 Set up the coarse model in the ADS schematic; set up the SM surrogate models as (4), (6), (8) or (10); set up the optimization and goals components (matching the magnitude of S11, etc.); set up parameter sweep to sweep the base set; set up the DAC component to read the base set point values from the database file; set up S2PMDIF to read the fine model responses.

Step 3 Simulate (optimize) the coarse model (SM-based surrogate) to match the fine model at all base points using the ADS optimization algorithm. This is the *Parameter extraction* step. Update the model.

Step 4 Deactivate optimization and goals.

Step 5 Generate random test points and save in a test set database file; set up the fine model simulator; simulate using the test set; save the responses in MDIF files.

Step 6 Revise the parameter sweep, DAC and S2PMDIF components in the schematic to load the test set of values and responses.

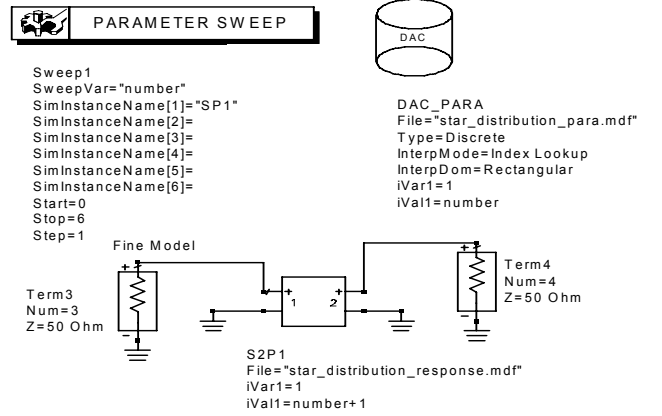*Step* 7 Simulate and compare the responses.

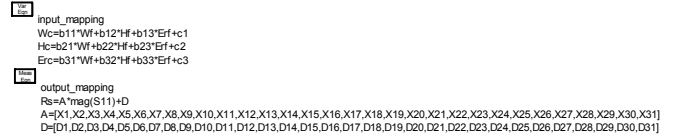Fig. 1. The ADS schematic setup of the fine model imported from Sonnet *em*.

Fig. 2. The SM surrogate setup in ADS. VAR component input_mapping deals with $\overline{B}$, $\overline{c}$. MeasEqn component output_mapping involves mapping parameters $\overline{A}$ and $\overline{d}$.

Now we can use the surrogate after deleting or deactivating the parameter sweep, DAC and S2PMDIF with its terminals from the schematic. We can apply the parameters to the surrogate as a new model. The model is easily switched between R_{s1}, R_{s2}, R_{s3} and R_{s4} by changing the SM surrogates in the MeasEqn (output_mapping as in Fig. 2). For R_{s1} we set Rs = mag(S11), for R_{s2}, Rs = A*mag(S11), for R_{s3}, Rs = mag(S11)+D, and for R_{s4}, Rs = A*mag(S11)+D.

IV. EXAMPLES

In this section we illustrate the implementation into the ADS framework of the models introduced in Section II. The models are set up using $2n+1$ base points (*n* is the number of design variables) as described in Section II. For each example, we perform a statistical analysis of the model error using the set of test points randomly chosen in the region of interest (with uniform distribution). The error is measured as an l_2 norm of the difference between the fine and the surrogate model responses. It is worth mentioning that we always restrict ourselves to on-grid points in Sonnet *em* for the base and test sets.

A. Microstrip Right-Angle Bend [5]

The design parameters of the microstrip right-angle bend are the width *W*, the substrate height *H* and the dielectric constant ε_r (See Fig. 3). The region of interest is $20\text{mil} \leq W \leq$

30mil, 8mil $\leq H \leq$ 16mil and $8 \leq \varepsilon_r \leq 10$. The frequency range is 1 GHz to 31 GHz with a step of 2 GHz (16 points). The number of base points in the region of interest is 7. The reference point is $\boldsymbol{x}^0 = [25\ 12\ 9]^T$, the region size $\boldsymbol{\delta} = [5\ 4\ 1]^T$.

We develop an Agilent ADS empirical model for the microstrip right-angle bend in Fig. 3(a). The fine model is analyzed by Sonnet's $\boldsymbol{em}^{TM}$ using 1mil × 1mil mesh size and the circuit model is the LC circuit shown in Fig. 3(b). The equivalent circuit parameters are calculated from expressions developed by Kirschning, Jansen and Koster according to their formula in [12].

Table I shows the statistical analysis of the modeling error for 10 random test points. Figs. 4 and 5 show error plots for the coarse model $\boldsymbol{R}_c$ and surrogate model $\boldsymbol{R}_{s4}$, respectively. Fig. 6 shows $|S_{11}|$ versus frequency for the fine model (−), the coarse model (×), and the $\boldsymbol{R}_{s2}$ model (o) for one test point.

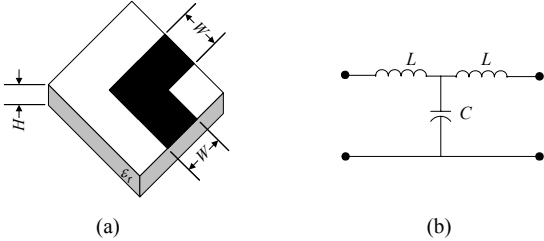(a)   (b)

Fig.3. The microstrip right-angle bend: (a) the fine model, (b) the circuit model.

TABLE I
ERROR STATISTICS FOR MICROSTRIP RIGHT-ANGLE BEND USING 10 RANDOM TEST POINTS IN THE REGION OF INTEREST

Model	Mean Error	Maximum Error
$\boldsymbol{R}_c$	0.345	0.428
$\boldsymbol{R}_{s1}$	0.022	0.030
$\boldsymbol{R}_{s2}$	0.012	0.030
$\boldsymbol{R}_{s3}$	0.011	0.027
$\boldsymbol{R}_{s4}$	0.011	0.029

B. Microstrip Shaped T-junction [5]

In this example we consider a shaped T-junction [5] (Fig. 7(a)). The T-junction is symmetric in the sense that all input lines have the same width w. The fine model is analyzed by Sonnet's $\boldsymbol{em}$ and the coarse model is composed of empirical models of simple microstrip elements (see Fig. 7(b)) of Agilent ADS. The fine and coarse model parameters are given by $\boldsymbol{x}_f = [w\ w_2\ w_1\ y\ x\ h\ \varepsilon_r]^T$ and $\boldsymbol{x}_c = [w_c\ w_{c2}\ w_{c1}\ y_c\ x_c\ h_c\ \varepsilon_{rc}]^T$. The region of interest is 15mil $\leq h \leq$ 25mil, 5mil $\leq x \leq$ 15mil, 5mil $\leq y \leq$ 15mil, and $8 \leq \varepsilon_r \leq 10$. The frequency range used is 2 GHz to 20 GHz with a step of 2 GHz (10 points). The width w of the input lines is determined in terms of h and ε_r so that the characteristic impedance of the input lines is 50 ohm. The width w_1 is taken as 1/3 of the width w. The width w_2 is obtained so that the characteristic impedance of the microstrip line after the step connected to port 2 is twice the characteristic impedance of the microstrip line after the step connected to port 1 (see Fig. 7(b)). The number of base points

in the region of interest is 9 since we have only 4 independent variables $\{h, x, y, \varepsilon_r\}$. The reference point is $\boldsymbol{x}^0 = [21\ 33\ 7\ 10\ 10\ 20\ 9]^T$.
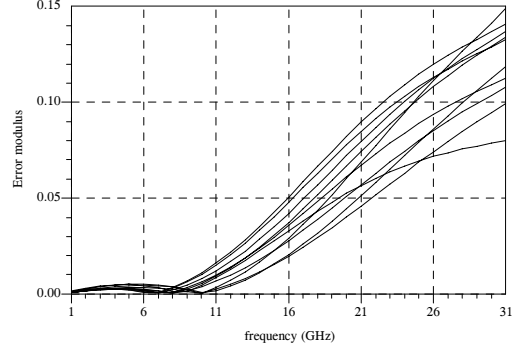

Fig. 4. Error plots for the $\boldsymbol{R}_c$ model (modulus of difference between $\boldsymbol{R}_f$ and $\boldsymbol{R}_c$) for the microstrip right-angle bend (10 test points).
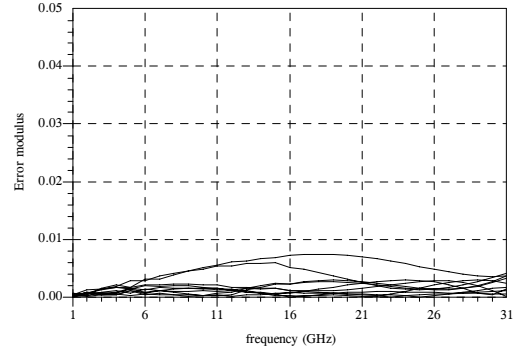
Fig.5. Error plots for the $\boldsymbol{R}_{s4}$ model (modulus of difference between $\boldsymbol{R}_f$ and $\boldsymbol{R}_{s4}$) for the microstrip right-angle bend (10 test points).
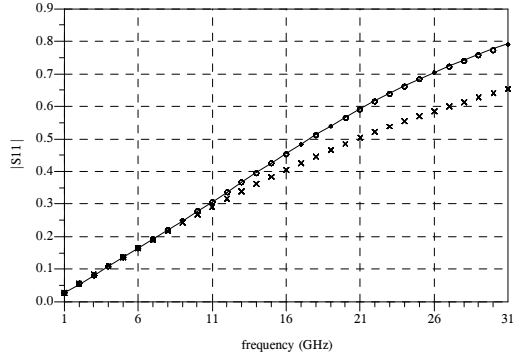

Fig. 6. $|S_{11}|$ for the microstrip right-angle bend: the fine model (−), the coarse model (×), and the $\boldsymbol{R}_{s2}$ model (o) at a test point.
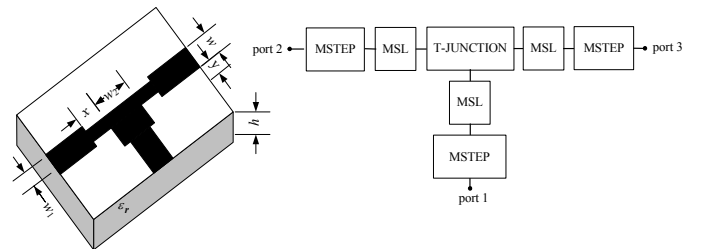

Fig. 7. Microstrip shaped T-junction: (a) the physical structure (fine model); (b) the coarse model.

3

Table II shows the statistical analysis of the modeling error for 24 random test points. Figs. 7 and 8 show error plots for the coarse model $\mathbf{R}_c$ and surrogate model $\mathbf{R}_{s4}$, respectively. Fig. 9 shows $|S_{11}|$ and $|S_{22}|$ versus frequency for the fine model (−), coarse model (×), and the $\mathbf{R}_{s2}$ model (o) at one test point.

TABLE II
ERROR STATISTICS FOR MICROSTRIP SHAPED T-JUNCTION USING 24
RANDOM TEST POINTS IN THE REGION OF INTEREST

Model	Mean Error	Maximum Error
$\mathbf{R}_c$	0.1481	0.207
$\mathbf{R}_{s1}$	0.0075	0.014
$\mathbf{R}_{s2}$	0.0062	0.013
$\mathbf{R}_{s3}$	0.0053	0.011
$\mathbf{R}_{s4}$	0.0052	0.010

(a)   (b)
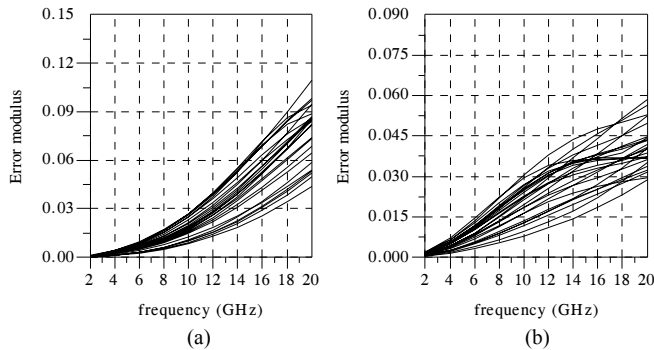
Fig. 7. Error plots for the $\mathbf{R}_c$ model (modulus of difference between $\mathbf{R}_f$ and $\mathbf{R}_c$) for the microstrip shaped T-junction (24 test points); (a) $|S_{11}|$; (b) $|S_{22}|$.
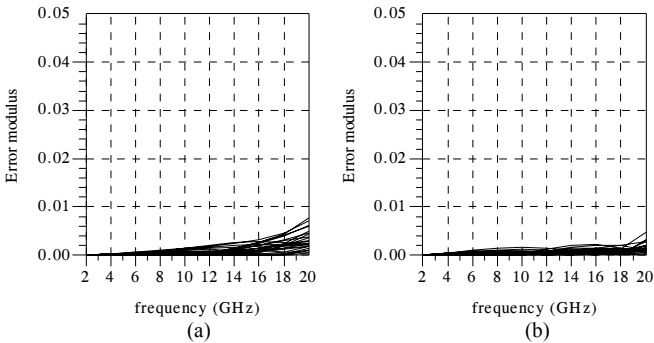

(a)   (b)

Fig. 8. Error plots for the $\mathbf{R}_{s4}$ model (modulus of difference between $\mathbf{R}_f$ and $\mathbf{R}_{s4}$) for the microstrip shaped T-junction (24 test points); (a) $|S_{11}|$; (b) $|S_{22}|$.
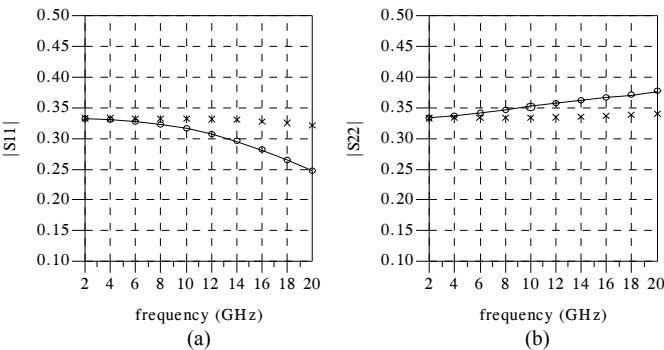

(a)   (b)

Fig. 9. $|S_{11}|$ and $|S_{22}|$ for the microstrip shaped T-junction: the fine model (−), the coarse model (×), and the $\mathbf{R}_{s2}$ model (o) at a test point.

V. CONCLUSIONS

We present an SM-based surrogate methodology for RF and microwave CAD, implemented and verified entirely in ADS. We show that it is easy to switch between the surrogates in the ADS schematic. The models offer good accuracy, much better in our examples than the models on which they are based.

REFERENCES

[1] J.W. Bandler, R.M. Biernacki, S.H. Chen, P.A. Grobelny and R.H. Hemmers, "Space mapping technique for electromagnetic optimization," *IEEE Trans. Microwave Theory and Tech.*, vol. 42, pp. 2536–2544, Dec. 1994.

[2] J.W. Bandler, R.M. Biernacki, S.H. Chen, R.H. Hemmers and K. Madsen, "Electromagnetic optimization exploiting aggressive space mapping," *IEEE Trans. Microwave Theory and Tech.*, vol. 43, pp. 2874–2882, Dec. 1995.

[3] J.W. Bandler, Q.S. Cheng, S.A. Dakroury, A.S. Mohamed, M.H. Bakr, K. Madsen and J. Søndergaard, "Space mapping: the state of the art," *IEEE Trans. Microwave Theory and Tech.*, vol. 52, pp. 337–361, Jan. 2004.

[4] M.H. Bakr, J.W. Bandler and N. Georgieva, "Modeling of microwave circuits exploiting space derivative mapping," in *1999 IEEE MTT-S Int. Microwave Symp. Dig.*, Anaheim, CA, June 1999, pp. 715–718.

[5] J.W. Bandler, N. Georgieva, M.A. Ismail, J.E. Rayas-Sánchez and Q. J. Zhang, "A generalized space mapping tableau approach to device modeling," *IEEE Trans. Microwave Theory and Tech.*, vol. 49, pp. 67–79, Jan. 2001.

[6] J.W. Bandler, M.A. Ismail, J.E. Rayas-Sánchez and Q.J. Zhang, "Neuromodeling of microwave circuits exploiting space mapping technology," *IEEE Trans. Microwave Theory and Tech.*, vol. 47, pp. 2417–2427, Dec. 1999.

[7] L. Zhang, J.J. Xu, M. Yagoub, R.T. Ding and Q.J. Zhang, "Neuro-space mapping technique for nonlinear device modeling and large signal simulation," in *2003 IEEE MTT-S Int. Microwave Symp. Dig.,* Philadelphia, PA, June 2003, pp. 173–176.

[8] Agilent ADS, Version 2003A, Agilent Technologies, 1400 Fountaingrove Parkway, Santa Rosa, CA 95403-1799, 2003.

[9] J.W. Bandler, Q.S. Cheng, D. Gebre-Mariam, K. Madsen, F. Pedersen and J. Søndergaard, "EM-based surrogate modeling and design exploiting implicit, frequency and output space mappings," in *2003 IEEE MTT-S Int. Microwave Symp. Dig.*, Philadelphia, PA, June 2003, pp. 1003–1006.

[10] J.W. Bandler, Q.S. Cheng, D.M. Hailu, and N.K. Nikolova, "A space mapping design framework," *IEEE Trans. Microwave Theory Tech.*, vol. 52, pp. 2601–2610, Nov. 2004.

[11] *em*™ Version 9.52, Sonnet Software, Inc., 100 Elwood Davis Road, North Syracuse, NY 13212, USA.

[12] M. Kirschning, R. H. Jansen, and N. H. L. Koster, "Measurement and computer-aided modeling of microstrip discontinuities by an improved resonator method," in *1983 IEEE MTT-S Int. Microwave Symp. Dig.*, Boston, MA, 1983, pp. 495–497.